Soft Matter

PAPER

Site-specific growth of polymers on silica rods†

Bo Peng,*[a] Giuseppe Soligno,[b] Marlous Kamp,[a] Bart de Nijs,[a] Joost de Graaf,[a] Marjolein Dijkstra,[a] René van Roij,[b] Alfons van Blaaderen*[a] and Arnout Imhof*[a]

Cite this: *Soft Matter*, 2014, **10**, 9644

Received 4th September 2014
Accepted 13th October 2014

DOI: 10.1039/c4sm01989j

www.rsc.org/softmatter

Colloids specifically developed for self-assembly (SA) into advanced functional materials have rapidly become more complex, as this complexity allows for more ways to optimize both the SA process and the properties of the resulting materials. For instance, by creating 'patchy' particles more open structures can be achieved through directional interactions. However, the number of ways in which site-specific chemistry can be achieved on particle surfaces is still limited. Here, we show how polymer patches can be specifically grown onto only the flat end of bullet-shaped silica rods by utilizing a subtle anisotropy in surface tension and shape caused by the growth mechanism of the rods. Conversely, if the bullet-shaped silica rods are used as 'Pickering-emulsion' stabilizers the same surface tension effects exclusively direct the orientation of the rods into a 'hedgehog-morphology'. Finally, we demonstrate how an external electric field can direct the particles in a 'vectorial' way.

1. Introduction

Considerable attention has been paid in recent years to colloidal particles that combine an anisotropic shape with a composite structure, because they combine the properties of different materials in one particle and allow anisotropy in materials properties. This leads to potential applications that are hard to achieve by either the materials alone or with spherically shaped particles, such as in the fabrication of optical, electronic, and sensing devices or as fillers for the paint and coating industries.[1–8] In addition, if the symmetry of the particles can be broken along the direction of the anisotropy, the resulting particles can in principle be pointed in specific directions with an external electric field. For instance, in the case of photo-catalytic rod-like particles that split water into its elemental components this would allow more easy separation of the oxygen and hydrogen produced by such systems.[9–11] Furthermore, the anisotropic interactions between such particles could be exploited in new collective assembly strategies, such as amphiphilic behaviour seen in particles composed of parts with varying hydrophilicity or surface roughness and liquid crystalline behaviour.[12–14] Much effort has been devoted to the synthesis and self-assembly of anisotropic hybrid particles, *e.g.* small clusters of spherical or dumbbell-shaped particles,[15–17] oriented surface modification of spheres placed on a substrate or interface,[18–20] or directed nucleation on the surface of primary particles.[21–23] Oriented surface modification has also been used to provide silica rods with gold tips.[24] Such so-called Janus rods have also been prepared by combining conventional lithography with nanorod synthesis[25–27] and by electroplating in an anodic alumina membrane.[28] Moreover, reactive ion etching of polymer rods out of a multilayer polymer film using colloidal particles as masks[29] has been demonstrated. These multistep procedures yield well-defined rods, but in small quantities.

Recently, our group developed a method to produce monodisperse rod-shaped silica colloids by droplet-induced directional growth of silica *via* the hydrolysis and condensation of a silica precursor.[30] The cylindrical particles grow out of water-in-oil emulsion droplets containing polyvinylpyrrolidone (PVP) and end up with one rounded end, where the silica growth started, and one flat end to which the droplet remained stably attached. This remarkable manner of attachment is exemplified by the fact that the rods could be elongated by further additions of the silica precursor.[30] Indeed, He *et al.*[31,32] produced amphiphilic silica rods in this way by post-addition of a second organo-silica precursor.

After the rods were removed from their original reaction mixture the water droplets disappeared and there was only slight anisotropy of the shape on both ends of the rod. We recently checked if the asymmetry in the ends gives rise to directionality of the rods in nematic and smectic liquid crystal phases formed by these bullet-shaped particles. This turned out not to be the case as was demonstrated by particles for which the fluorescence intensity was not constant over the length of the rods.[33]

[a]*Soft Condensed Matter, Debye Institute for Nanomaterials Science, Utrecht University, Princetonplein 5, 3584 CC Utrecht, The Netherlands. E-mail: pengbo006@gmail.com; A.vanBlaaderen@uu.nl; A.Imhof@uu.nl*

[b]*Institute for Theoretical Physics, Center for Extreme Matter and Emergent Phenomena, Utrecht University, Leuvenlaan 4, 3584 CE Utrecht, The Netherlands*

† Electronic supplementary information (ESI) available: Details about experimental methods and adsorption free energy calculations. See DOI: 10.1039/c4sm01989j

Here, we used these particles, after surface modification with a silane coupling agent containing the monomer of polymethylmethacrylate (PMMA), as seeds in a typical dispersion polymerization (of methylmethacrylate (MMA) or styrene (St)). We found that the polymer bulbs that formed at the ends of the rods became attached exclusively at the end where once the water droplet had been. Interesting hybrid organic–inorganic colloids with anisotropic properties in the direction of the length of the rod can be produced in this manner. We investigated the cause of the preferred attachment by tuning the shape and surface chemistry of the rods and we are now able to control the attachment site. Furthermore, we found that the silica rods could also replace the usual polymeric steric stabilizer in dispersion polymerization by collectively attaching end-on to the surfaces of growing PMMA particles, as in a Pickering emulsion. Particles with a unique hedgehog-like (or porcupine-like) architecture were produced in this way. Finally, we performed free-energy calculations to determine the stability of these hedgehog-like assemblies.

2. Results and discussion

2.1. Synthesis

Several batches of silica rods were synthesized following the method from our previous work (details can be found in the ESI†).[30] A typical monodisperse silica rod system with a diameter (D) of 327 nm and a length (L) of 1.2 μm is shown in the inset of Fig. 1a. The 3D reconstruction of the particle shape, achieved by electron tomography,[34,35] clearly shows the bullet-like shape and the difference between the two ends of the rods, one of which is hemispherical while the other is almost flat. In order to use these particles as seeds their surfaces were first modified with the silane coupling agent trimethoxysilyl propyl methacrylate (TPM). A typical one-pot dispersion polymerization of the monomer in a polar medium was then carried out: all the agents (TPM modified silica rods, PVP as a stabilizer, initiator, monomer (MMA or St) and solvent) were added to a flask and dispersed homogeneously under a nitrogen stream. Elevation of the temperature then initiated the polymerization. Details of the synthesis and purification are given in the ESI.† Interestingly, the obtained hybrid particles exhibited a lollipop shape due to the exclusive attachment of the polymer bulbs to the less curved tips of the rods. Typical systems are shown in Fig. 1b–d (for PMMA) and S1† (for PS). The growth location of the polymer bulbs was independent of the aspect ratio (from 1.9 to 5.8) of the rods. The concentration ratio of monomer to seed particles also did not influence the growth location, but only the size of the polymer bulb. The recipe was not yet optimized to prevent secondary nucleation of PMMA, however this did not attach to the silica rods and could be easily removed by centrifugation. Upon increasing the amount of reactants in the synthesis, the yield was readily scaled up and the obtained particles possessed a good uniformity in shape (see ESI and Fig. S1a†).

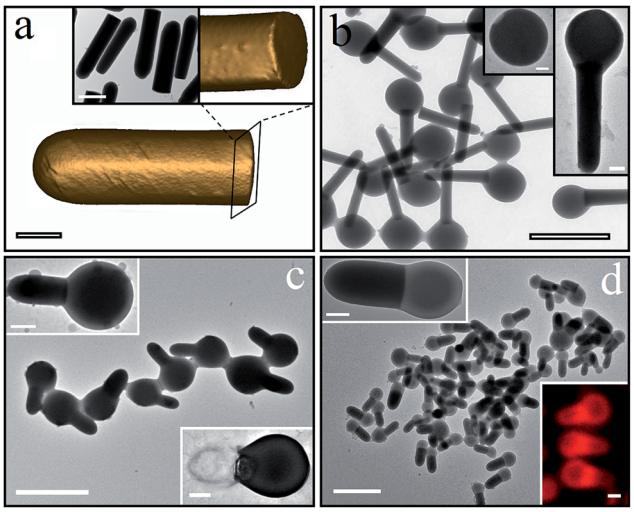

Fig. 1 Transmission electron microscopy (TEM) images of the hybrid silica–PMMA particles. (a) 3D reconstruction using electron tomography of a single silica rod showing that the two ends have different curvatures. The insets show a close-up of the flat end and a TEM image of the silica rods (L = 1.2 μm and D = 327 nm). (b) TEM images of 'lollipop-shaped' particles made from long rods (L = 1.3 μm and D = 225 nm). The PMMA bulbs (D_{PMMA} = 940 nm) only attached at the flat end of the rods. The insets show an occasional detached PMMA bulb that displays a clear indentation and a single hybrid particle at higher resolution. (c) TEM image of lollipop-shaped particles (D_{PMMA} = 868 nm) made from short rods (L = 737 nm and D = 384 nm) at a mass ratio of 9.7 : 1. The insets show a single particle at a higher resolution and the result of etching the silica seed with HF. (d) A similar result (D_{PMMA} = 603 nm) at a lower mass ratio between MMA and silica rods of 4.85 : 1. The lower inset shows the as-synthesized particles after fluorescent labelling in a solvent matching the refractive index of silica. The scale bar in a is 200 nm and 500 nm in the inset. The scale bars in (b–d) are 2 μm and 200 nm in the insets.

2.2. Exploration of the formation mechanism

We monitored in more detail the formation of the PMMA bulbs at the flat ends in the sample of Fig. 1c by taking samples at different times during the preparation. The samples were quenched in a large amount of room-temperature solvent to

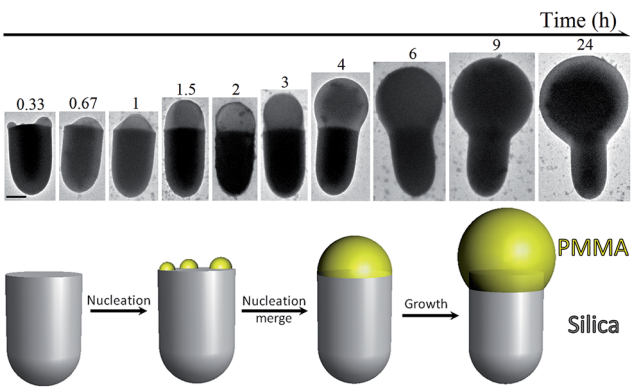

Fig. 2 TEM images, taken at intervals, of the attachment and growth of a PMMA bulb onto the flat end of the silica rods. The lower row shows a cartoon of the process. The scale bar is 200 nm.

prevent further growth. TEM images of these samples are shown in Fig. 2 (also see Fig. S2 and S3†). It is clear that PMMA nuclei are mainly present on the flat end of the silica already early in the reaction (see Fig. S2†). However, small side-on and edge-on nuclei were also found (see the insets in Fig. S2†). A little while later only end-on nuclei appeared, and these nuclei were seen to have merged (see Fig. S3†), after which a PMMA bulb grew until the monomer ran out. The contact line between the PMMA and silica appeared to be pinned at the edge of the silica bullet, *i.e.*, the bulb does not 'spill over' much onto the side of the rod, leading to a relatively large droplet and giving the particle its distinctive lollipop shape.

In order to investigate why the PMMA so strongly prefers to attach to the flat ends several additional experiments were performed. The commonly used surface coating with the silane coupling agent TPM strongly promotes the nucleation of dispersion-polymerized PMMA on silica, but it is expected to cover the whole silica surface. The necessity of TPM treatment was seen from an experiment in which this step was omitted: no association between the PMMA and silica was observed at all and separate PMMA spheres were formed instead (see Fig. S4†). A surface treatment with TPM (or similar compound) is what allows spherical silica seeds to be partially wetted by PS so that they can be decorated with one or more polymer bulbs.[2,22] Fig. S5† shows such a result using our exact synthesis protocol. Alternatively, if the silica surface is wetted completely by the PMMA, the silica becomes covered with a complete and uniform layer: this is shown in Fig. S6† where a dispersion polymerization in an apolar medium (hexane/dodecane) was used in conjunction with a comb-graft stabilizer of polyhydroxystearic acid grafted onto PMMA (for details see ESI†), similarly as already described for the coating of silica spheres.[36]

Two reasons can be put forward to explain the exclusive attachment of PMMA to the flat silica ends: the first is a lower surface free energy for nucleation of a hemispherical monomer-swollen PMMA droplet at a flat surface as compared to a rounded surface. A second possible explanation is that the surface chemistry of the flat silica end differs from that of the rest of the surface. During the silica synthesis this end remained in contact with the water droplet, which contained a high concentration of PVP and sodium citrate,[30] and could therefore contain different amounts of organic residues. For example, from elemental analysis and porosimetry we know that a small percentage of PVP is actually incorporated into the silica.[33] It is conceivable, then, that the flat silica end contains more PVP than the other surfaces. Such an excess quantity is too small, however, to detect with analytical methods.

The surface chemistry of the rods can be made more uniform by coating them with an additional thin layer of silica with the usual seeded Stöber growth method (for experimental details see ESI†).[37] When a 15 nm coating was applied, the edges of the silica rods also became slightly rounded, but their original shape was largely preserved. After the usual TPM treatment this thin silica coating was enough to direct part of the PMMA toward the sides of the silica rods (see Fig. 3 and S7†). A further increase of the silica coating to ~150 nm led to two ends with

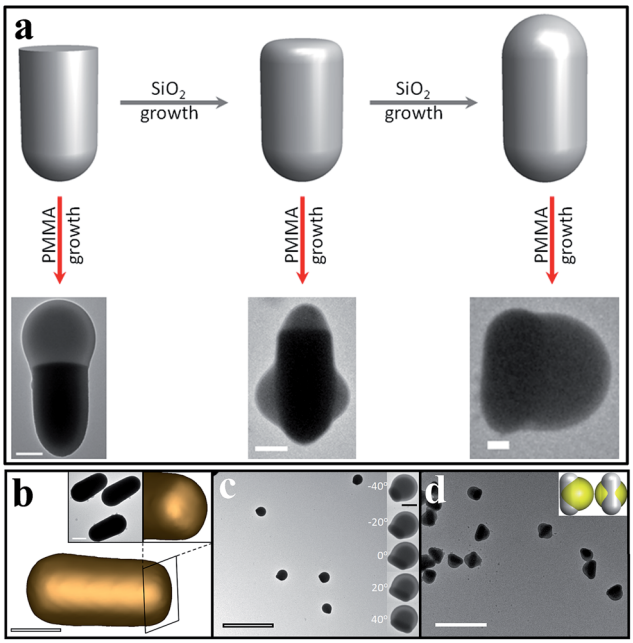

Fig. 3 Control over the PMMA bulb growth location. (a) Attachment of the PMMA bulb to silica rods that have been coated with an additional layer of 0, 15, and 150 nm of silica. The silica–MMA mass ratio was 9.7 : 1. (b) 3D electron tomography reconstruction of a single silica rod with two rounded ends due to a 150 nm coating. (c) TEM images of rods (two identical ends, $L = 1.7$ μm, and $D = 0.78$ μm) with a PMMA bulb ($D = 2.04$ μm) attached to the side of each rod. The insets show a single hybrid particle observed from different viewing angles at a high resolution. (d) TEM images of hybrid particles at a lower mass ratio of 4.85 : 1. The insets show schematic images of these hybrid particles at different viewing angles. The scale bar is 200 nm, 500 nm, 10 μm and 5 μm in (a, b, c and d), and 500 nm and 1 μm in the insets of (b and d), respectively.

nearly the same curvature. This time PMMA formed a single bulb, but it attached to the silica rod side-on. This experiment suggests that the surface heterogeneity principally determines the location of the PMMA attachment. However, since the thickness of the silica coating still seems to influence the PMMA distribution a shape effect cannot be excluded.

A way to remove any surface heterogeneity with little change in the shape of the silica seeds is a 24 hour treatment with piranha solution. This is expected to remove any organic residues and to result in a uniform hydroxylated silica surface. However, we found that most, but not all, PMMA was still attached to the ends of the silica rods (see Fig. S8†). Alternatively, a calcination step at 500 °C is expected to certainly remove all organics. After further re-hydroxylation and TPM coating steps the PMMA this time attached to the edge of the rods (see Fig. S9†). Although the calcination also caused a slight rounding of the silica edge the particle shape was largely preserved. The most likely explanation for the PMMA attachment location therefore seems to be a different surface chemistry of the flat ends as the dominant effect, with perhaps some additional influence of the particle shape. Moreover, these experiments present useful ways to manipulate the morphology of hybrid organic–inorganic particles.

2.3. Silica rods as colloidal stabilizers

The 'perfect' (meaning 100% effective) site-specific attachment of PMMA to the as-synthesized silica rods suggests that they could conversely serve to stabilize these polymer particles by a mechanism similar to that in a Pickering emulsion.[38] In recent years, it has been shown that rod and disk shaped particles can also efficiently stabilize emulsion droplets or foam bubbles, by attaching solely side-on to them.[39–41] On the other hand, our silica rods are expected to attach end-on to the PMMA, which would be quite unique. Therefore, we again performed a dispersion polymerization of MMA in the presence of TPM-modified silica rods, but this time omitted PVP as the steric stabilizer (for details see the ESI†). First, rods with a flat tip and an aspect ratio of 1.9 were used at a silica : MMA weight ratio of 1 : 4.85. Nearly monodisperse hedgehog-shaped hybrid particles were obtained, as shown in Fig. 4a and b. From these images, one can indeed distinguish that only the flat ends attached to the PMMA phase, as expected, covering the whole PMMA surface. The fact that the PMMA is present as separate particles shows that the bullet-shaped silica rods successfully played their role as a shape-anisotropic steric stabilizer. A similar result was obtained with longer rods (Fig. 4c), where a smaller amount of PMMA (silica : MMA = 1 : 2.43 in mass) was stabilized. Also, in accordance with our earlier observations rods with two rounded ends were all attached side-on (Fig. 4d), and the stabilized quantity of monomer further decreased to one fifth the amount of the short rod system (silica : MMA = 1 : 0.97).

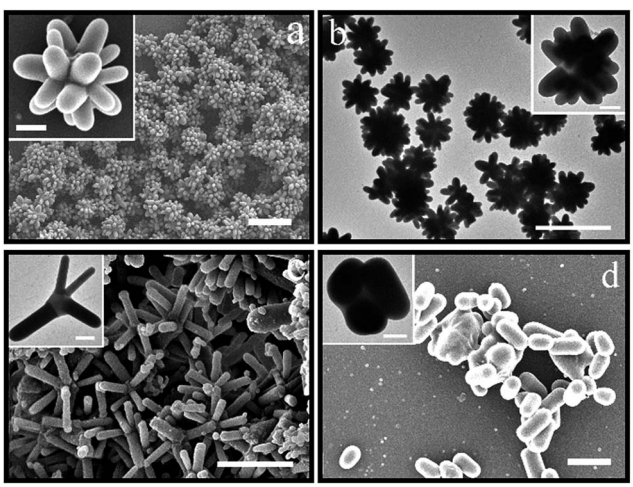

Fig. 4 PMMA particles stabilized by silica rods instead of PVP during synthesis as a Pickering emulsion. (a–c) PMMA stabilized by 100% flat-end attachment: 'hedgehog configuration'. (a) SEM and (b) TEM images of short rods (aspect ratio of 1.9) stabilizing PMMA colloids prepared at a silica to MMA mass ratio of 1 : 4.85. (c) SEM image of long rods (aspect ratio of 4.2) stabilizing the PMMA at a mass ratio of 1 : 2.43. The inset shows a TEM image. (d) SEM image of rods (aspect ratio of 2.2, coated with extra silica to produce two rounded ends) stabilizing PMMA at a mass ratio of 1 : 0.97. The inset shows a TEM image. The scale bars are 5 μm in (a and b) and 2 μm in (c and d), and 500 nm in the insets, respectively.

2.4. Adsorption free-energy calculations

Experiment and theory have shown that the preferred orientation of attachment of a cylinder to a fluid interface is determined by the length-to-diameter ratio and the contact angle of the cylinder.[42] In order to better understand the mechanism behind the observed phenomena and get a better idea of the generality of the approach we discovered with our silica rods, we numerically analysed the adsorption free energy of a single bullet-shaped rod with homogeneous surface properties at a flat liquid-liquid interface shown in Fig. 4a and b by using a triangular-tessellation technique and employing reasonable estimates of the surface tensions between silica, (liquid) PMMA and methanol (see ESI† for the method used).[43–46] The results are shown in Fig. S12 and 13.† The planar interface can be used to model the adsorption of a particle to a spherical droplet, when the curvature of the droplet is not too small, and can therefore be employed to gain insight into the stability of the observed hedgehog assemblies. According to the minimum adsorption free energy, a side-on configuration of surface-homogeneous silica particles attached to the PMMA phase is more favorable than the flat end-on configuration. However, the flat end-on configuration is a metastable state, separated from the global minimum by a high energy barrier (several hundred k_BT). This means that once the rod attaches to the PMMA with its flat end, thermal fluctuations are insufficient to change that situation. This is true even when very low interfacial tensions (down to 0.1 mN m^{-1}) are assumed. In this case, the exclusive presence of the end-on configuration in the hedgehog-like structures could be related to the experimentally observed preference of the PMMA to nucleate on the flat end of the silica bullets, thus favouring an initial metastable state which is preserved during the PMMA growth. The complete absence of rods that lie flat on the interface in the experiment, however, raises the question whether rods without a PMMA bulb, could orient themselves perpendicular to the interface upon adsorbing, as an initial contact with the interface that would result in adsorption to the equilibrium configuration (side-on) is quite likely.[44] That is, are there parameters for which the bullets can absorb to the PMMA end-on in a stable way, with the side-on attachment being unstable/metastable? The preferential nucleation of PMMA at the flat end of the bullets indicates that there may be surface heterogeneities, which contribute to the behaviour of these colloids. Therefore, we included a surface chemical heterogeneity into our model by giving the flat side of the rod a different contact angle (θ_1) than the rest of its surface (θ_0). As shown in Fig. 5a, two distinct minimum energy orientation regions (blue and red) emerged in which the bullet-shaped rods prefer to stand up on the interface. This straight-up orientation becomes favourable when the contact angles are sufficiently different (away from the diagonal in Fig. 5a), in particular when $|\cos\theta_0| > 0.3$, *i.e.*, when the rounded (non-flat) surface is either sufficiently wettable or sufficiently non-wettable with respect to PMMA. A reduction of the contact angle is then seen to lower the energy minimum for end-on attachment below that for side-on attachment (Fig. 5b and c). For instance, the following combinations of the surface tensions: $\gamma_{1sg} - \gamma_{2sg} = -4.2 \times 10^{-5}$

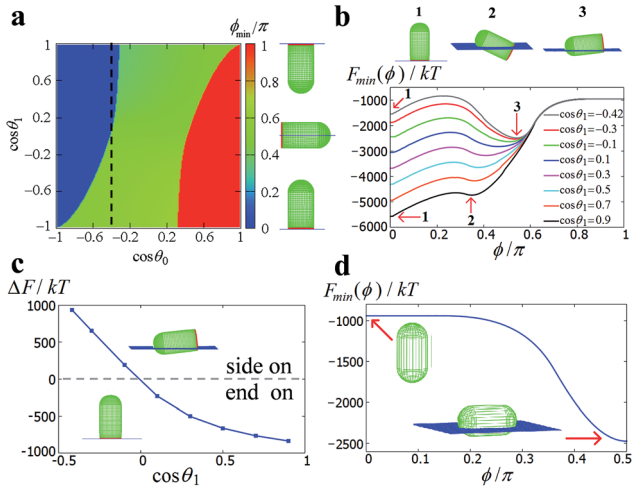

Fig. 5 Adsorption free-energy calculations of rod-shaped particles at an interface. (a) Contour plot of the minimum free-energy orientation of the rods (aspect ratio is 1.9) where the colour coding refers to the polar angle ϕ (between the interface normal and the rotational symmetry axis of the particle, also see Fig. S11a†) as indicated graphically on the right, as a function of the cosine of the contact angles θ_1 (the flat base of the bullet rods, shown in red) and θ_0 (the remaining surface). (b) Orientation dependence of the free energy (minimized with respect to the distance from the interface) for a bullet-shaped rod adsorbed at the interface and various flat-end contact angles θ_1 taken along the dashed line where $\cos\theta_0 = -0.42$. (c) Free-energy difference between the end-on configuration and side-on configuration of a bullet-shaped rod ($L = 737$ nm and $D = 384$ nm) as a function of the flat-end contact angle for $\cos\theta_0 = -0.42$ fixed. (d) Orientation-dependence of the free energy of adsorption (minimised with respect to the distance from the interface) for a spherocylindrical rod (aspect ratio is 2.2, as in Fig. 3d and 4d, no flat end) for $\cos\theta_0 = -0.42$, showing only a side-on equilibrium configuration. $1\ kT = 4.11 \times 10^{-21}$ N m.

N m^{-1} and $\gamma_{1sr} - \gamma_{2sr} \geq -1.5 \times 10^{-6}$ N m^{-1} (the subscripts 1, 2, s, r and g refer to liquid 1, 2, solid, at the red (flat) surface and at the green (rest) surface (see Fig. 5), 1 is the solvent and 2 is the droplet, and γ_{12} is adopted as 0.0001 N m^{-1}, for details see the ESI†), would result in the flat attachment becoming stable. In addition, this reduced contact angle on the flat end of the bullet with respect to that on the shaft, is also observed in the experiment. The sample in the inset of Fig. S2† shows a bullet to which two polymer bulbs are attached at different sites. The figure clearly indicates that for this system θ_1 is much lower than θ_0, which provides strong evidence of the validity of our model. We therefore conclude that heterogeneity in surface chemistry may indeed play an important role in the formation and stability of the observed hedgehog assemblies. A similar conclusion was reached for rods of aspect ratio 4.2 (for details see Fig. S15–17†). For the rods with two rounded ends (spherocylinder-like silica rods) and without surface heterogeneity, used in Fig. 4d, only a side-on attachment possesses the minimum energy (see Fig. 5d). This explains why no colloidal hedgehogs are observed for this system and only PMMA droplets with rods attached side-on were found. Also, the calculation results of end-on to side-on attachment in our model are consistent with the experimental observation in Fig. 3a, which proves the validity of our model. Despite the fact that the triangular-tessellation-based calculations do not model the process of nucleation of small droplets, it is tempting to relate the above adsorption-based results to the mechanism of PMMA nucleation, which occurs exclusively at the flat end of the bullet-shaped rods and does not occur for spherocylindrical rods (see Fig. 1 and 3d). Indeed, surface heterogeneities probably play an important role in this nucleation, as indicated by the experimental findings combined with our theoretical analysis. However, further studies of this more complicated problem are required before a definitive theoretical determination of the effect of local surface heterogeneities and curvature (shape) on the nucleation and growth of PMMA can be made. That is to say, the assumption of a planar fluid–fluid interface in our model, could lead to quantitatively (and possibly qualitatively) different results than if we had modeled the adsorption to a droplet with radius comparable to the size of the bullet. Indeed, Zeng *et al.*[47] pointed out that for a spherical particle the consequences of the interfacial curvature can be significant. However, a similar calculation for our bullet shaped particle is exceedingly complex and therefore goes beyond the scope of the current investigation.

2.5. Vectorial alignment of the lollipop particles

The one-sided attachment of PMMA onto the bullet-shaped rods allows them to be uniformly directed by an electric field, as illustrated in Fig. S10 (for details see the ESI†). The same was not possible for the silica rods alone.[33] Presently, research is ongoing to determine what is the most important contribution to this vectorial alignment as several factors (charge on the rods, double-layer thickness, and dielectric polarizability differences) possibly all contribute to this effect.

3. Conclusions

In conclusion, hybrid silica–polymer particles were prepared *via* a typical dispersion polymerization in which the locus of the attachment of the polymer onto the silica rod could be controlled. At an early stage of the reaction the polymer nuclei preferentially attached to the flat end of the bullet-shaped silica rods, after which they grew to form a single spherical bulb there. Upon modification of these rods by growing extra silica layers or calcination, the location of polymer attachment could be shifted from end-on to side-on. We used this preferred attachment to produce PMMA particles from which multiple silica rods protrude perpendicularly like the spines of a hedgehog. Theoretical calculations show that the attachment location and stability of the rods to the hedgehog can be explained in terms of a difference in surface chemistry between the flat end and the shaft of the silica rods, while the geometry mainly acts to trap the polymer. The broken symmetry in terms of material properties of our particles along the length direction also makes it possible to vectorially direct the individual particles with external fields, which may have important implications for the self-assembly behaviour of these particles.

4. Experimental section

4.1. End-on attachment of polymers to silica rods

Lollipop-shaped polymer–silica colloids were synthesized through a multi-step approach, which involved bullet-shaped silica rod synthesis, surface modification of rods, and polymer growth in a dispersion polymerization. The details are described in the ESI.†

4.2. Side-on attachment of polymers to silica rods

In order to shift the attachment of the polymer to the rods from end-on to side-on, the surface of rods was made chemically homogeneous prior to surface decoration with TPM, either through coating with extra silica layers or calcination (the details are provided in the ESI†). Subsequently, the monomer became grafted onto the side of the rods in a typical dispersion polymerization in the presence of the stabilizer and thermal initiator.

4.3. Colloidal silica rods as stabilizers

The silica rods can also play the role of the chemical surfactant in our system, which sets our system apart from classical dispersion polymerization. Typically, TPM modified silica rods were dispersed in methanol along with the initiator; after a deoxygenation step, the elevation of temperature started the polymerization. The structure of products mainly depended on the surface properties and geometry of the rods.

4.4. Adsorption free-energy calculations

Adsorption free-energy calculations were performed using a so-called triangular-tessellation technique, in which the surface of the particles was approximated by a large number of triangles. In this model, only one rod-shaped particle adsorbed to the flat interface between two liquids was considered. The free energy of adsorption is governed by the surface area that results from contact between the various media. The details can be found in the ESI.†

Acknowledgements

C. Schneijdenberg and J. D. Meeldijk are thanked for assistance with the SEM and TEM measurements and J. Stiefelhagen and A. Kuijk are thanked for helpful discussions. B. Peng thanks Nanodirect EU FP7-NMP-2007-SMALL-1, project 213948 for financial support. G. Soligno, M. Kamp and B. de Nijs acknowledge financial support from "Nederlandse Organisatie voor Wetenschappelijk Onderzoek" (NWO) for Vici, ECHO and CW grants, respectively. G. Soligno and R. van Roij also thank the Marie Curie Initial Training Network "Soft Matter at Aqueous Interfaces" (SOMATAI) for financial support. This work is part of the DITP consortium, a program of the NWO that is funded by the Dutch Ministry of Education, Culture and Science (OCW). J. de Graaf acknowledges financial support from the High Potential Program of Utrecht University.

Notes and references

1 S. Glotzer and M. Solomon, *Nat. Mater.*, 2007, **6**, 557.
2 E. Duguet, A. Desert, A. Perro and S. Ravaine, *Chem. Soc. Rev.*, 2011, **40**, 941.
3 J. Hu, S. Zhou, Y. Sun, X. Fang and L. Wu, *Chem. Soc. Rev.*, 2012, **41**, 4356.
4 A. Perro, S. Reculusa, S. Ravaine, E. Bourgeat-Lami and E. Duguet, *J. Mater. Chem.*, 2005, **15**, 3745.
5 S. Yan, S. Kim, J. Lim and G. Yi, *J. Mater. Chem.*, 2008, **18**, 2177.
6 A. Walther and A. H. Muller, *Soft Matter*, 2008, **4**, 663.
7 A. Kumar, B. J. Park, F. Tu and D. Lee, *Soft Matter*, 2013, **9**, 6604.
8 S. Jiang, Q. Chen, M. Tripathy, E. Luijten, K. S. Schweizer and S. Granick, *Adv. Mater.*, 2010, **22**, 1060.
9 X. Chen, S. Shen, L. Guo and S. Mao, *Chem. Rev.*, 2010, **110**, 6503.
10 A. Kubacka, M. Fernandez-Garcia and G. Colon, *Chem. Rev.*, 2012, **112**, 1555.
11 L. Amirav and A. P. Alivisatos, *J. Phys. Chem. Lett.*, 2010, **1**, 1051.
12 J.-W. Kim, D. Lee, H. C. Shum and D. A. Weitz, *Adv. Mater.*, 2008, **20**, 3239.
13 D. J. Kraft, R. Ni, F. Smallenburg, M. Hermes, K. Yoon, D. A. Weitz, A. van Blaaderen, J. Groenewold, M. Dijkstra and W. K. Kegel, *Proc. Natl. Acad. Sci.*, 2012, **109**, 10787.
14 G. J. Vroege and H. N. W. Lekkerkerker, *Rep. Prog. Phys.*, 1992, **55**, 1241.
15 Y. Yin, Y. Lu, B. Gates and Y. Xia, *J. Am. Chem. Soc.*, 2001, **123**, 8718.
16 D. Zerrouki, J. Baudry, D. Pine, P. Chaikin and J. Bibette, *Nature*, 2008, **455**, 380.
17 B. Peng, F. Smallenburg, A. Imhof, M. Dijkstra and A. van Blaaderen, *Angew. Chem., Int. Ed.*, 2013, **52**, 6709.
18 V. N. Paunov and O. J. Cayre, *Adv. Mater.*, 2004, **16**, 788.
19 Y. Lu, H. Xiong, X. Jiang and Y. Xia, *J. Am. Chem. Soc.*, 2003, **125**, 12724.
20 M. A. Correa-Duarte, V. Salgueirino-Maceira, B. Rodriguez-González, L. M. Liz-Marzán, A. Kosiorek, W. Kandulski and M. Giersig, *Adv. Mater.*, 2005, **17**, 2014.
21 A. Perro, E. Duguet, O. Lambert, J.-C. Taveau, E. Bourgeat-Lami and S. Ravaine, *Angew. Chem., Int. Ed.*, 2009, **48**, 361.
22 A. Ohnuma, E. C. Cho, P. H. C. Camargo, L. Au, B. Ohtani and Y. Xia, *J. Am. Chem. Soc.*, 2009, **131**, 1352.
23 S. Sacanna, L. Rossi and D. J. Pine, *J. Am. Chem. Soc.*, 2012, **134**, 6112.
24 K. Chaudhary, Q. Chen, J. J. Juarez, S. Granick and J. A. Lewis, *J. Am. Chem. Soc.*, 2012, **134**, 12901.
25 L. Qin, S. Park, L. Huang and C. A. Mirkin, *Science*, 2005, **309**, 113.
26 C. Choi, J. Lee, K. Yoon, A. Tripathi, H. A. Stone, D. A. Weitz and C. Lee, *Angew. Chem., Int. Ed.*, 2010, **49**, 7748.
27 J. Wang, Y. Wang, S. S. Sheiko, D. E. Betts and J. M. DeSimone, *J. Am. Chem. Soc.*, 2012, **134**, 5801.

28 Y. Wang, R. M. Hernandez, D. J. Bartlett, J. M. Bingham, T. R. Kline, A. Sen and T. E. Mallouk, *Langmuir*, 2006, **22**, 10451.
29 X. Li, T. Wang, J. Zhang, D. Zhu, X. Zhang, Y. Ning, H. Zhang and B. Yang, *ACS Nano*, 2010, **4**, 4350.
30 A. Kuijk, A. van Blaaderen and A. Imhof, *J. Am. Chem. Soc.*, 2011, **133**, 2346.
31 J. He, M. J. Hourwitz, Y. Liu, M. T. Perez and Z. Nie, *Chem. Commun.*, 2011, **47**, 12450.
32 J. He, B. Yu, M. J. Hourwitz, Y. Liu, M. T. Perez, J. Yang and Z. Nie, *Angew. Chem., Int. Ed.*, 2012, **51**, 3628.
33 A. Kuijk, A. Imhof, M. H. W. Verkuijlen, T. H. Besseling, E. R. H. Van Eck and A. van Blaaderen, *Part. Part. Syst. Charact.*, 2014, **31**, 706.
34 J. R. Kremer, D. N. Mastronarde and J. R. McIntosh, *J. Struct. Biol.*, 1996, **116**, 71.
35 D. N. Mastronarde, *J. Struct. Biol.*, 1997, **120**, 343.
36 W. K. Kegel and A. van Blaaderen, *Science*, 2000, **287**, 290.
37 W. Stöber, A. Fink and E. Bohn, *J. Colloid Interface Sci.*, 1968, **26**, 62.
38 S. U. Pickering, *J. Chem. Soc., Trans.*, 1907, **91**, 2001.
39 P. F. Noble, O. J. Cayre, R. G. Alargova, O. D. Velev and V. N. Paunov, *J. Am. Chem. Soc.*, 2004, **126**, 8092.
40 A. F. Bon and P. J. Colver, *Langmuir*, 2007, **23**, 8316.
41 W. Zhou, J. Cao, W. Liu and S. Stoyanov, *Angew. Chem., Int. Ed.*, 2009, **48**, 378.
42 E. P. Lewandowski, P. C. Searson and K. J. Stebe, *J. Phys. Chem. B*, 2006, **110**, 4283.
43 J. de Graaf, M. Dijkstra and R. van Roij, *Phys. Rev. E: Stat., Nonlinear, Soft Matter Phys.*, 2009, **80**, 051405.
44 J. de Graaf, M. Dijkstra and R. van Roij, *J. Chem. Phys.*, 2010, **132**, 164902.
45 M. P. Arciniegas, M. R. Kim, J. de Graaf, R. Brescia, S. Marras, K. Miszta, M. Dijkstra, R. van Roij and L. Manna, *Nano Lett.*, 2014, **14**, 1056.
46 W. van der Stam, A. P. Gantapara, Q. A. Akkerman, G. Soligno, J. D. Meeldijk, R. van Roij, M. Dijkstra and C. de Mello Donega, *NanoLett.*, 2014, **14**, 1032.
47 C. Zeng, F. Brau, B. Davidovitch and A. D. Dinsmore, *Soft Matter*, 2012, **8**, 8582.